Ain Shams Engineering Journal (2016) xxx, xxx–xxx

Ain Shams University

Ain Shams Engineering Journal

www.elsevier.com/locate/asej
www.sciencedirect.com

ENGINEERING PHYSICS AND MATHEMATICS

Darcy–Forchheimer flow of hydromagnetic nanofluid over a stretching/shrinking sheet in a thermally stratified porous medium with second order slip, viscous and Ohmic dissipations effects

N. Vishnu Ganesh [a], A.K. Abdul Hakeem [a,*], B. Ganga [b]

[a] Department of Mathematics, Sri Ramakrishna Mission Vidyalaya College of Arts and Science, Coimbatore 641 020, India
[b] Department of Mathematics, Providence College for Women, Coonoor 643 104, India

Received 26 October 2015; revised 19 March 2016; accepted 29 April 2016

KEYWORDS

Darcy–Forchheimer flow;
Nanofluid;
Ohmic dissipation;
Second order slip;
Thermally stratified medium

Abstract A boundary layer analysis is carried out to study the influences of second order slip, viscous and Ohmic dissipations on steady two dimensional, incompressible flow of water based nanofluid over a stretching/stretching sheet embedded in a thermally stratified porous medium with inertia effect in the presence of magnetic field. The governing boundary layer nonlinear PDEs are transformed into nonlinear ODE's using scaling transformation. The transformed equations are solved numerically by the fourth order Runge–Kutta method with shooting technique. Moreover, analytical solutions are presented for a special case. A unique solution is obtained for stretching sheet and dual solutions are found for shrinking sheet which depend on the suction parameter and local inertia coefficient. The effects of physical parameters on the dual solutions, temperature profile, local skin friction coefficient and the reduced Nusselt number are discussed. Comparisons are found to be good with benchmark solution.

1. Introduction

The improvement of heat transfer performance is very much important in the view of energy conservation in a system. Conventional heat transfer fluids such as water and oils have limitation in enhancing the performance and the compactness of systems because of its low thermal conductivity. The thermal conductivity of the solids is higher than liquids. An innovative and new technique to augment heat transfer is to use solid particles in the base fluid (i.e. nanofluids) in the range of sizes 10–50 nm. Abu-Nada et al. [1] analyzed the natural convection heat transfer enhancement in horizontal concentric annuli filled by nanofluid. Due to nanofluids wide applicability in biomedical, optical and electronic fields, considerable interest has been in the nanofluid boundary flow problems [2–22].

* Corresponding author.
E-mail address: abdulhakeem6@gmail.com (A.K. Abdul Hakeem).
Peer review under responsibility of Ain Shams University.

ELSEVIER Production and hosting by Elsevier

http://dx.doi.org/10.1016/j.asej.2016.04.019

Numerous industrial and environmental systems including geothermal energy systems, fibrous insulation, heat exchanger design, geophysics, and catalytic reactors involve the convection flow through porous media. The non-Darcian porous medium model is an extension of the classical Darcian model which includes vorticity diffusion, tortuosity inertial drag effects and combinations of these effects [23]. The Darcy–Forchheimer (DF) model is probably the most popular modification to Darcian flow utilized in similarity inertia effects. Inertia effect is accounted through the inclusion of a velocity squared term in the momentum equation, which is known as Forchheimer's extension. Pal and Mondal [24,25] considered the non-Darcy Forchheimer's flow model over a stretching surface in their publications. Recently, Anwar et al. [26] studied the Darcy Forchheimer's flow over a moving vertical surface in a thermally stratified medium in ordinary fluids.

The study of magnetic field effects has important applications in physics, chemistry and engineering. Industrial equipment, such as magnetohydrodynamic (MHD) generators, pumps, bearings and boundary layer control are affected by the interaction between the electrically conducting fluid and a magnetic field [27,28]. Viscous dissipation is quite often a negligible effect, but its contribution might become important when the fluid viscosity is very high. It changes the temperature distributions by playing a role like an energy source, which leads to affected heat transfer rates. Anjali devi and Ganga [29] studied the effects of viscous and Joules dissipation on MHD flow past a stretching porous surface embedded in a porous medium for ordinary fluid. The effects of thermal radiation and viscous dissipation on boundary layer flow of nanofluids over a moving flat plate were studied in [30,31]. Very recently, Ganga et al. [32] investigated the viscous and Ohmic dissipations on magnetohydrodynamic radiative flow of nanofluid over a vertical plate in the presence of internal heat generation/absorption.

In micro-electro mechanical systems the fluid flow behavior does not obey the no-slip boundary condition because of the micro-scale-dimension of the devices and also when the fluid is particulate such as emulsions, foams, polymer solutions and suspensions the no slip condition is not-suitable. Keeping this in view, second order slip effects on the fluid flow over a stretching/shrinking surface have been analyzed by [33–36]. Rosca and Pop [37] investigated the effect of second order slip on boundary layer flow of micropolar fluid over a shrinking sheet. Very recently, Abdul Hakeem et al. [38] studied the second order slip effects on MHD flow of water based nanofluid over stretching/shrinking surface in the presence of thermal radiation.

As per author's knowledge no work has been done in the problem of second order slip flow and heat transfer of non-Darcy radiative flow of nanofluid over a stretching/shrinking surface with viscous and Ohmic dissipations. This fact motivates us to suggest the same for the present investigation. The governing boundary layer nonlinear partial differential equations are transformed into nonlinear ordinary differential equations using scaling transformation. The transformed equations are solved numerically by the fourth order Runge–Kutta method with shooting technique.

2. Mathematical formulation

Consider the steady, laminar, two-dimensional, radiative incompressible viscous water based nanofluid flow over stretching/shrinking sheet embedded in a saturated non-Darcian porous medium with viscous and Ohmic dissipations in the presence of internal heat generation/absorption. A uniform magnetic field of strength of B_0 applied normally to the sheet. The magnetic Reynolds number is assumed to be small so that the induced magnetic field can be neglected. The sheet is of temperature $T_w(\bar{x})$ and is embedded in a thermally

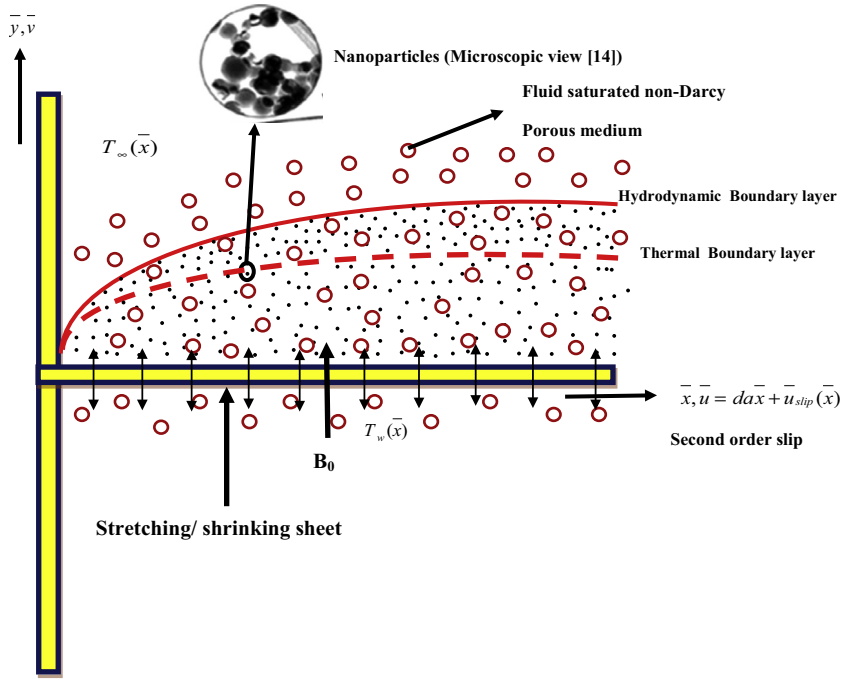

Fig. 1 Physical model and the co-ordinate system of the problem.

stratified medium of variable ambient temperature $T_\infty(\bar{x})$ where $T_w(\bar{x}) > T_\infty(\bar{x})$. It is assumed that $T_w(\bar{x}) = T_0 + b\bar{x}$ and $T_\infty(\bar{x}) = T_0 + c\bar{x}$. Where T_0 is the reference temperature, $a, b > 0$ and $c \geqslant 0$ are constants. The fluid is a water based nanofluid containing different types of spherical metallic [gold (Au), copper (Cu), silver (Ag) and aluminum (Al)] and non-metallic [aluminum oxide (Al_2O_3) and titanium oxide (TiO_2)] nanoparticles. It is assumed that the nanofluid experiences a second order slip at the sheet surface and also it is assumed that the base fluid and the nanoparticles are in thermal equilibrium and no slip occurs between them (see Fig. 1). The thermo physical properties of the nanofluid are considered as [38] (Table 1). The continuity, momentum and energy equations governing the above stated problem under usual boundary layer approximation are written as

$$\frac{\partial \bar{u}}{\partial \bar{x}} + \frac{\partial \bar{v}}{\partial \bar{y}} = 0, \tag{1}$$

$$\bar{u}\frac{\partial \bar{u}}{\partial \bar{x}} + \bar{v}\frac{\partial \bar{u}}{\partial \bar{y}} = \left(\frac{\mu_{nf}}{\rho_{nf}}\right)\frac{\partial^2 \bar{u}}{\partial \bar{y}^2} - \frac{\mu_{nf}\bar{u}}{\rho_{nf}k} - \frac{C_b}{\sqrt{k}}\bar{u}^2 - \frac{\sigma B_0^2 \bar{u}}{\rho_{nf}}, \tag{2}$$

$$\bar{u}\frac{\partial T}{\partial \bar{x}} + \bar{v}\frac{\partial T}{\partial \bar{y}} = \frac{k_{nf}}{(\rho C_p)_{nf}}\frac{\partial^2 T}{\partial \bar{y}^2} + \frac{Q}{(\rho c_p)_{nf}}(T - T_\infty) + \frac{\mu_{nf}}{(\rho C_p)_{nf}}\left(\frac{\partial \bar{u}}{\partial \bar{y}}\right)^2 + \frac{\sigma B_0^2 \bar{u}^2}{(\rho C_p)_{nf}} - \frac{1}{(\rho C_p)_{nf}}\frac{\partial q_r}{\partial \bar{y}}, \tag{3}$$

where $\bar{x}$ is the coordinate along the sheet, $\bar{u}$ is the velocity component in the $\bar{x}$ direction, $\bar{y}$ is the coordinate perpendicular to the sheet, $\bar{v}$ is the velocity component in the $\bar{y}$ direction, k is the permeability of the porous medium, C_b is the form of drag coefficient which is only depended on the geometry of the medium and independent of other physical properties of the fluid. The second and third terms on the right hand side of momentum equation stand for the first-order (Darcy) resistance and second-order porous inertia resistance, respectively. The constant $C_b/\sqrt{k}$ is called the Forchheimer number. The momentum equation is reduced to Darcy's law if the Forchheimer number equals to zero. In the energy equation, T is the local temperature of the fluid, T_∞ is the temperature of the fluid far away from the sheet, Q is the temperature-dependent volumetric rate of heat source when $Q > 0$ and heat sink when $Q < 0$ dealing with the situations of exothermic and endothermic chemical reactions respectively and q_r is the radiative flux.

Using Rosseland approximation for radiation (see Abdul Hakeem et al. [39]) we have

$$q_r = -\frac{4\sigma^*}{3k^*_{nf}}\frac{\partial T^4}{\partial \bar{y}}. \tag{4}$$

Table 1 Thermo-physical properties of water and nanoparticles [40].

	ρ (kg/m^3)	C_p (J/kg K)	k (W/m K)
Pure water	997.1	4179	0.613
Gold (Au)	19,300	132	296
Silver (Ag)	10,500	235	429
Copper (Cu)	8933	385	401
Aluminum (Al)	2710	913	201
Aluminum oxide (Al_2O_3)	3970	765	40
Titanium oxide (TiO_2)	4250	686.2	8.9538

Here, σ^* is the Stefan–Boltzmann constant and k^*_{nf} is the absorption coefficient of the nanofluid. Further, we assume that the temperature difference within the flow is such that T^4 may be expanded in a Taylor series. Hence, expanding T^4 about T_∞ and neglecting higher order terms we get,

$$T^4 \cong 4T_\infty^3 T - 3T_\infty^4. \tag{5}$$

Therefore Eq. (3) is simplified to

$$\bar{u}\frac{\partial T}{\partial \bar{x}} + \bar{v}\frac{\partial T}{\partial \bar{y}} = \frac{k_{nf}}{(\rho C_p)_{nf}}\frac{\partial^2 T}{\partial \bar{y}^2} + \frac{Q}{(\rho c_p)_{nf}}(T - T_\infty) + \frac{\mu_{nf}}{(\rho C_p)_{nf}}\left(\frac{\partial \bar{u}}{\partial \bar{y}}\right)^2 + \frac{\sigma B_0^2 \bar{u}^2}{(\rho C_p)_{nf}} + \frac{16\sigma^* T_\infty^3}{3k^*_{nf}(\rho C_p)_{nf}}\frac{\partial^2 T}{\partial \bar{y}^2}, \tag{6}$$

where ρ_{nf} is the effective density of the nanofluid, μ_{nf} is the effective dynamic viscosity of the nanofluid, $(\rho C_p)_{nf}$ is the heat capacitance and k_{nf} is the thermal conductivity of the nanofluid are given as [8,38]

$$\rho_{nf} = (1-\phi)\rho_f + \phi\rho_s, \quad \mu_{nf} = \frac{\mu_f}{(1-\phi)^{2.5}}, \tag{7}$$

$$(\rho C_p)_{nf} = (1-\phi)(\rho C_p)_f + \phi(\rho C_p)_s, \tag{8}$$

$$k_{nf} = k_f\left\{\frac{k_s + 2k_f - 2\phi(k_f - k_s)}{k_s + 2k_f + \phi(k_f - k_s)}\right\}. \tag{9}$$

Here, ϕ is the solid volume fraction.

The boundary conditions of Eqs. (1)–(3) are

$$\bar{u} = da\bar{x} + \bar{U}_{slip}, \quad \bar{v} = \bar{v}_w(\bar{x}), \quad T = T_w(\bar{x}) \text{ at } \bar{y} = 0,$$
$$\bar{u} \to 0, \quad T \to T_\infty \text{ as } \bar{y} \to \infty, \tag{10}$$

where $d = 1$ denotes stretching and $d = -1$ denotes shrinking sheets, respectively. a is a constant, $\bar{U}_{slip}$ is the slip velocity at the wall and v_w is the wall mass transfer velocity. The Wu's second order slip velocity model (valid for arbitrary Knudsen numbers, K_n) [33,34] is given by

$$\bar{U}_{slip} = \frac{2}{3}\left(\frac{3-\alpha l^3}{\alpha} - \frac{3}{2}\frac{1-l^2}{K_n}\right)\lambda\frac{\partial \bar{u}}{\partial \bar{y}} - \frac{1}{4}\left[l^4 + \frac{2}{K_n^2}(1-l^2)\right]\lambda^2\frac{\partial^2 \bar{u}}{\partial \bar{y}^2} = A\frac{\partial \bar{u}}{\partial \bar{y}} + B\frac{\partial^2 \bar{u}}{\partial \bar{y}^2}, \tag{11}$$

where $l = \min[1/K_n, 1]$, α is the momentum accommodation coefficient with $0 \leqslant \alpha \leqslant 1$ and λ is the molecular mean free path. Based on the definition of l, it is noticed that for any given value of K_n, we have $0 \leqslant l \leqslant 1$. The molecular mean free path is always positive. Thus we know that $B < 0$ and hence the second term in right hand side of Eq. (11) is a positive number.

By introducing the following non-dimensional variables

$$x = \frac{\bar{x}}{\sqrt{\frac{\nu_f}{a}}}, \quad y = \frac{\bar{y}}{\sqrt{\frac{\nu_f}{a}}}, \quad u = \frac{\bar{u}}{\sqrt{\nu_f a}}, \quad v = \frac{\bar{v}}{\sqrt{\nu_f a}}, \quad \theta = \frac{T - T_\infty}{T_w - T_0}. \tag{12}$$

Eqs. (1), (2) and (6) take the following non-dimensional form

$$\frac{\partial u}{\partial x}+\frac{\partial v}{\partial y}=0, \tag{13}$$

$$u\frac{\partial u}{\partial x}+v\frac{\partial u}{\partial y}=\frac{1}{\left(1-\phi+\phi\frac{\rho_s}{\rho_f}\right)}\left\{\frac{1}{(1-\phi)^{2.5}}\left(\frac{\partial^2 u}{\partial y^2}-k_1 u\right)-Mn\,u\right\} -\frac{C_b\sqrt{v_f}}{\sqrt{ka}}u^2, \tag{14}$$

$$u\frac{\partial\theta}{\partial x}+v\frac{\partial\theta}{\partial y}=\left(\frac{3N+4}{3N}\right)\left(\frac{k_{nf}}{k_f Pr}\right)\frac{1}{\left((1-\phi)+\phi\frac{(\rho C_p)_s}{(\rho C_p)_f}\right)}\frac{\partial^2\theta}{\partial y^2} +\frac{\lambda\theta}{\left((1-\phi)+\phi\frac{(\rho C_p)_s}{(\rho C_p)_f}\right)}+\frac{Ec\left(\frac{\partial u}{\partial y}\right)^2}{x^2(1-\phi)^{2.5}\left(1-\phi+\frac{(\rho Cp)s}{(\rho Cp)f}\right)} +\frac{MnEcu^2}{x^2\left(1-\phi+\frac{(\rho Cp)s}{(\rho Cp)f}\right)}-\frac{\theta u}{x}-\frac{cu}{bx}, \tag{15}$$

with the boundary conditions

$$u=dx+\gamma\frac{\partial u}{\partial y}+\delta\frac{\partial^2 u}{\partial y^2},\quad v=v_w,\quad T=T_w \text{ at } y=0,$$
$$u\to 0,\quad T\to T_\infty \text{ as } y\to\infty, \tag{16}$$

where $Pr=\frac{v_f}{\alpha_f}$ is the Prandtl number, $k_1=\frac{v_f}{ka}$ is the porous medium parameter, $Mn=\frac{\sigma B_0^2}{\alpha\rho_f}$ is the magnetic interaction parameter, $\lambda=\frac{Q}{(\rho C_p)_f a}$ is the heat source/sink parameter, $N=\frac{k_{nf}k^*_{nf}}{4\sigma^* T_\infty^3}$ is the radiation parameter, $Ec=\frac{u_w^2}{(Cp)_f}(T_w-T_o)$ is the Eckert number, γ is the first order velocity slip parameter with $0<\gamma=A\sqrt{a/v_f}$ and δ is the second order velocity slip parameter with $0>\delta=Ba/v_f$.

By introducing the stream function ψ, which is defined as $u=\frac{\partial\psi}{\partial y}$ and $v=-\frac{\partial\psi}{\partial x}$, then Eqs. (14) and (15) become

$$\frac{\partial\psi}{\partial y}\frac{\partial^2\psi}{\partial x\partial y}-\frac{\partial\psi}{\partial x}\frac{\partial^2\psi}{\partial y^2} =\frac{1}{\left(1-\phi+\phi\left(\frac{\rho_s}{\rho_f}\right)\right)}\left\{\frac{1}{(1-\phi)^{2.5}}\left(\frac{\partial^3\psi}{\partial y^3}-k_1\frac{\partial\psi}{\partial y}\right)-Mn\frac{\partial\psi}{\partial y}\right\} -\Gamma\left(\frac{\partial\psi}{\partial y}\right)^2, \tag{17}$$

$$\frac{\partial\psi}{\partial y}\frac{\partial\theta}{\partial x}-\frac{\partial\psi}{\partial x}\frac{\partial\theta}{\partial y} =\left(\frac{3N+4}{3N}\right)\left(\frac{k_{nf}}{k_f Pr}\right)\frac{1}{\left((1-\phi)+\phi\frac{(\rho C_p)_s}{(\rho C_p)_f}\right)}\frac{\partial^2\theta}{\partial y^2} +\frac{\lambda\theta}{\left((1-\phi)+\phi\frac{(\rho C_p)_s}{(\rho C_p)_f}\right)}+\frac{Ec\left(\frac{\partial^2\psi}{\partial y^2}\right)^2}{x^2(1-\phi)^{2.5}\left(1-\phi+\frac{(\rho Cp)s}{(\rho Cp)f}\right)} +\frac{MnEc\left(\frac{\partial\psi}{\partial y}\right)^2}{x^2\left(1-\phi+\frac{(\rho Cp)s}{(\rho Cp)f}\right)}-\frac{\partial\psi}{\partial y}\left(\frac{\theta}{x}-\frac{c}{bx}\right), \tag{18}$$

and the corresponding boundary conditions in Eq. (16) become

$$\frac{\partial\psi}{\partial y}=dx+\gamma\frac{\partial^2\psi}{\partial y^2}+\delta\frac{\partial^3\psi}{\partial y^3},\quad \frac{\partial\psi}{\partial x}=s,\quad T=T_w \text{ at } y=0,$$
$$\frac{\partial\psi}{\partial y}\to 0,\quad \theta\to 0 \text{ as } y\to\infty. \tag{19}$$

Now using the scaling group G of transformations, we get the scaling transformations

$$\eta=y,\quad \psi=xF(\eta),\quad \theta=\theta(\eta). \tag{20}$$

Now using the scaling group transformations in Eqs. (17) and (18) we get

$$F'''+c_2\left(FF''-(1+\Gamma)F'^2\right)-F'(c_1 Mn+k_1)=0, \tag{21}$$
$$\theta''+c_5(F\theta'-F'\theta)+c_4\lambda\theta=c_5F'St-c_4MnEcF'^2-c_6EcF''^2, \tag{22}$$

and the corresponding boundary conditions are

$$F=s,\quad F'=d+\gamma F''+\delta F''',\quad \theta=1-St \text{ at } \eta=0,$$
$$F'\to 0\quad \theta\to 0 \text{ as } \eta\to\infty. \tag{23}$$

where $\Gamma=\frac{C_b\sqrt{v_f}x}{\sqrt{ka}}$ is the local inertia coefficient, $St=c/b$ is the stratification parameter, $c_1=(1-\phi)^{2.5}$, $c_2=c_1\left(1-\phi+\phi\left(\frac{\rho_s}{\rho_f}\right)\right)$, $c_3=\left(1-\phi+\phi\frac{(\rho C_p)_s}{(\rho C_p)_f}\right)$, $c_4=\frac{3Nk_fPr}{k_{nf}(3N+4)}$, $c_5=c_3c_4$ and $c_6=c_4/c_1$.

3. An analytical treatment on flow field and heat transfer for a special case

It may be noted that the closed form solutions for the momentum equation can be found in the absence of local inertia coefficient i.e. $\Gamma=0$.

The exact solution to the differential Eq. (21) satisfying the boundary conditions in Eq. (23) in the absence of local inertia coefficient is obtained as

Table 2a Comparison of the values of $-F''(0)$ for stretching sheet.

γ	δ	Present results with $\phi=0$, $d=1$, $k_1=0$, $Mn=0$ and $s=2$		Turkyilmazoglu [35] with $Mn=0$, $k_1=0$, $\phi=0$ and $\Gamma=0$
		Analytical	Numerical	
0	−1	0.3894282565	0.3894282565	0.38942826
3	−3	0.1044918663	0.1044918663	0.10449187
5	−5	0.0642051113	0.0642051113	0.06420511

Table 2b Comparison of the values β for $d=-1$, $\phi=0$, $\Gamma=0$, $k_1=0$, $Mn=0$ and $\delta=-1$.

s	γ	Present results Analytical	Turkyilmazoglu [35] β
2^U	0	1.88320351	1.8832035
10^U	1	9.99909886	9.9990096
2^L	0	0.531010056	0.53101006
10^L	1	0.09173797	0.09173797

Please cite this article in press as: Vishnu Ganesh N et al., Darcy–Forchheimer flow of hydromagnetic nanofluid over a stretching/shrinking sheet in a thermally stratified porous medium with second order slip, viscous and Ohmic dissipations effects, Ain Shams Eng J (2016), http://dx.doi.org/10.1016/j.asej.2016.04.019

$$F(\eta) = s + \frac{d(1-e^{-\beta\eta})}{\beta(1+\gamma\beta-\delta\beta^2)}. \tag{24}$$

Substituting Eq. (24) in Eq. (21) gives the following fourth order algebraic equation for the characteristic parameter β with $\Gamma = 0$

$$dc_2 + (1+\gamma\beta-\delta\beta^2)[c_1 Mn + k_1 + \beta(c_2 s - \beta)] = 0. \tag{25}$$

The velocity profile for both stretching and shrinking surface is obtained as

$$F'(\eta) = \frac{de^{-\beta\eta}}{(1+\gamma\beta-\delta\beta^2)}. \tag{26}$$

The corresponding four roots of Eq. (24) are analytically expressed, respectively as

$$\begin{aligned}
\beta &= -\frac{-\gamma - c_2 s\delta}{4\delta} - \frac{\beta_1}{2} - \frac{\sqrt{\beta_2 - \beta_3}}{2},\\
\beta &= -\frac{-\gamma - c_2 s\delta}{4\delta} - \frac{\beta_1}{2} + \frac{\sqrt{\beta_2 - \beta_3}}{2},\\
\beta &= -\frac{-\gamma - c_2 s\delta}{4\delta} + \frac{\beta_1}{2} - \frac{\sqrt{\beta_2 + \beta_3}}{2},\\
\beta &= -\frac{-\gamma - c_2 s\delta}{4\delta} + \frac{\beta_1}{2} + \frac{\sqrt{\beta_2 + \beta_3}}{2},
\end{aligned} \tag{27}$$

where

$$\beta_1 = \sqrt{\frac{-2(-1+c_2 s\gamma - k_1\delta + c_1 Mn\delta)}{3\delta} + \frac{(-\gamma - c_2 s\delta)^2}{4\delta^2} + \frac{\beta_4}{3\delta\beta_5} + \frac{\beta_5}{3\delta 2^{1/3}}},$$

$$\beta_2 = \frac{-4(-1+c_2 s\gamma - k_1\delta - c_1 Mn\delta)}{3\delta} + \frac{(-\gamma - c_2 s\delta)^2}{2\delta^2} - \frac{\beta_4}{3\delta\beta_5} - \frac{\beta_5}{3\delta 2^{1/3}},$$

$$\beta_3 = \frac{\beta_7}{4\beta_1},$$

$$\beta_4 = 2^{1/3}(12(c_2 d + c_1 Mn + k_1)\delta + (-1+c_2 s\gamma - k_1\delta - c_1 Mn\delta)^2 - 3(c_2 s + k_1\gamma + c_1 Mn\gamma)(-\gamma - c_2 s\delta)),$$

$$\beta_5 = \left(\beta_6 + \sqrt{-4\left(\frac{\beta_4}{2^{1/3}}\right)^3 + \beta_6^2}\right)^{1/3},$$

$$\begin{aligned}
\beta_6 = {} & 27(c_2 s + k_1\gamma + c_1 Mn\gamma)^2\delta - 72(c_2 d + k_1 + c_1 Mn)\\
& \times \delta(-1+c_2 s\gamma - k_1\delta - c_1 Mn\delta) + 2(-1+c_2 s\gamma - k_1\delta - c_1 Mn\delta)^3\\
& - 9(c_2 s + k_1\gamma + c_1 Mn\gamma)(-1+c_2 s\gamma - k_1\delta - c_1 Mn\delta)(-\gamma - c_2 s\delta)\\
& + 27(c_2 d + k_1 + c_1 Mn)(-\gamma - c_2 s\delta)^2
\end{aligned}$$

and

$$\beta_7 = \frac{-8(c_2 s + k_1\gamma + c_1 Mn\gamma)}{\delta} + \frac{4(-1+c_2 s\gamma - k_1\delta - c_1 Mn\delta)(-\gamma - c_2 s\delta)}{\delta^2} - \frac{(-\gamma - c_2 s\delta)^3}{\delta^3}.$$

It should be mentioned that a unique solution exists for stretching sheet ($d = 1$) as given by the fourth of Eq. (27) and also the dual solutions which are called lower and upper branch solutions exist for shrinking sheet ($d = -1$) given by third and fourth of Eq. (27) respectively.

Thus the non-dimensional velocity components are

$$u = x\frac{de^{-\beta\eta}}{(1+\beta\gamma-\delta\beta^2)}, \quad v = -\left(s + \frac{d(1-e^{-\beta\eta})}{\beta(1+\beta\gamma-\delta\beta^2)}\right). \tag{28}$$

The dimension velocity components are

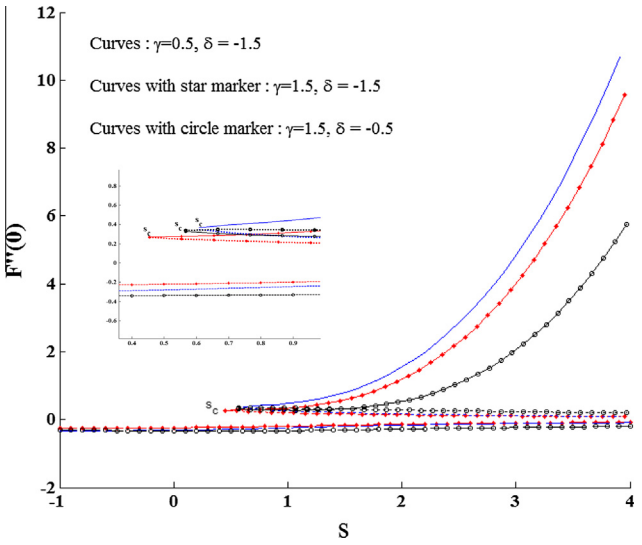

Fig. 2 Variations of $F''(0)$ for different values of s, γ and δ when $\Gamma = 0.5$, $k_1 = 0.4$, $Mn = 0.4$ and $\phi = 0.05$. (Dashed lines correspond to stretching sheet, dotted lines correspond to shrinking sheet upper branch solution and solid lines correspond to shrinking sheet lower branch solution).

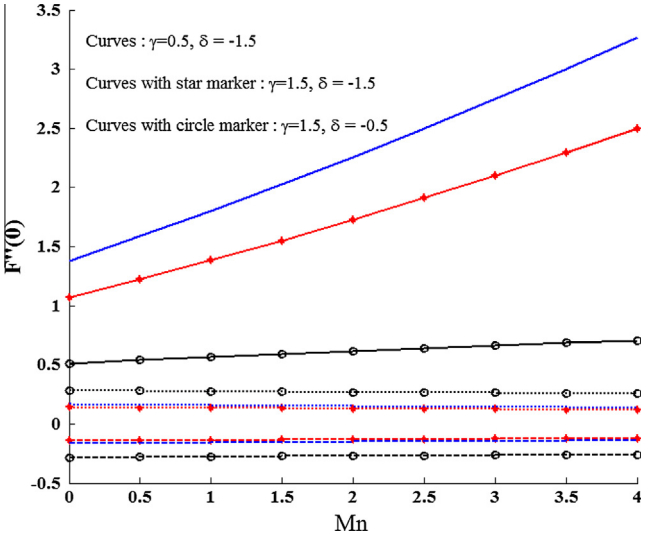

Fig. 3 Variations of $F''(0)$ for different values of Mn, γ and δ when $\Gamma = 0.5$, $k_1 = 0.4$, $s = 2$ and $\phi = 0.05$. (Dashed lines correspond to stretching sheet, dotted lines correspond to shrinking sheet upper branch solution and solid lines correspond to shrinking sheet lower branch solution).

$$\bar{u} = a\bar{x}\frac{de^{-\beta\sqrt{\frac{a}{\nu_f}}\bar{y}}}{(1+\beta\gamma-\delta\beta^2)}, \quad \bar{v} = -\sqrt{a\nu_f}\left(s + \frac{d(1-e^{-\beta\sqrt{\frac{a}{\nu_f}}\bar{y}})}{\beta(1+\beta\gamma-\delta\beta^2)}\right). \tag{29}$$

The shear stress at the stretching sheet characterized by the skin friction coefficient C_f, is given by

$$C_f = \frac{-2\mu_{nf}}{\rho_f(\bar{u}_w(\bar{x}))^2}\left(\frac{\partial\bar{u}}{\partial\bar{y}}\right)_{\bar{y}=0}. \tag{30}$$

Please cite this article in press as: Vishnu Ganesh N et al., Darcy–Forchheimer flow of hydromagnetic nanofluid over a stretching/shrinking sheet in a thermally stratified porous medium with second order slip, viscous and Ohmic dissipations effects, Ain Shams Eng J (2016), http://dx.doi.org/10.1016/j.asej.2016.04.019

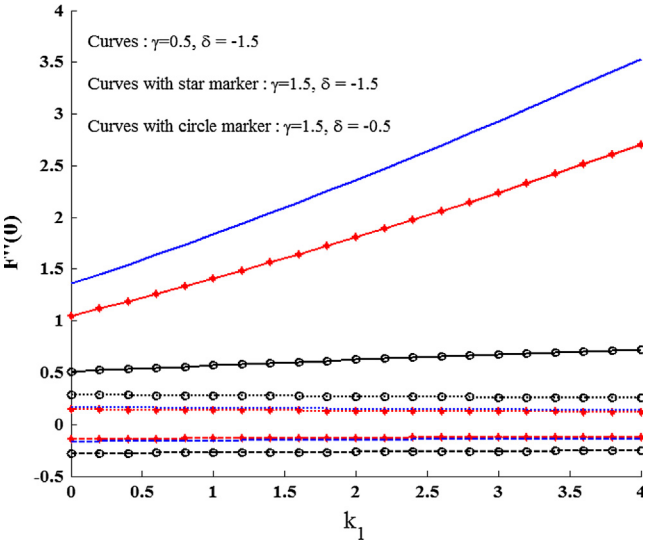

Fig. 4 Variations of $F''(0)$ for different values of k_1, γ and δ when $\Gamma = 0.5$, $Mn = 0.4$, $s = 2$ and $\phi = 0.05$. (Dashed lines correspond to stretching sheet, dotted lines correspond to shrinking sheet upper branch solution and solid lines correspond to shrinking sheet lower branch solution).

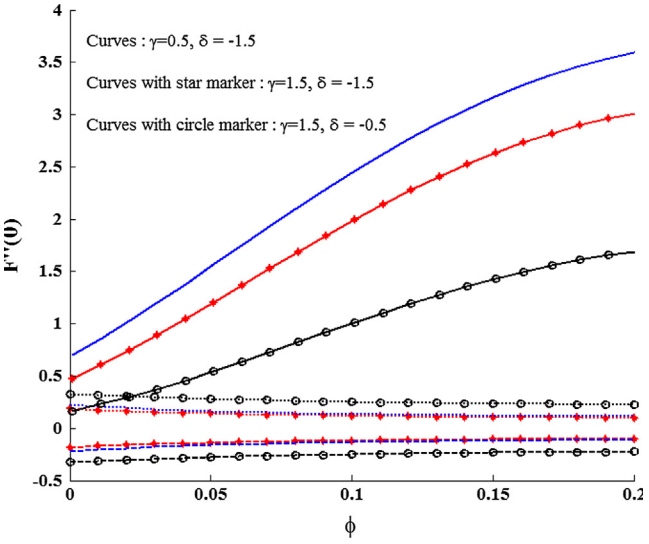

Fig. 5 Variations of $F''(0)$ for different values of ϕ, γ and δ when $\Gamma = 0.5$, $Mn = 0.4$, $s = 2$ and $k_1 = 0.4$. (Dashed lines correspond to stretching sheet, dotted lines correspond to shrinking sheet upper branch solution and solid lines correspond to shrinking sheet lower branch solution).

Using Eqs. (12), (20), (24) and (29), the skin friction can be written as

$$Re_x^{1/2} C_f = -\frac{2}{c_1} F''(0) = \frac{2}{c_1} \frac{d\beta}{(1+\gamma\beta-\delta\beta^2)}, \tag{31}$$

where $Re_x = \overline{x}\overline{u}_w(\overline{x})/v_f$ is the local Reynolds number based on the stretching velocity $\overline{u}_w(\overline{x})$ and $Re_x^{1/2} C_f$ is the local skin friction coefficient.

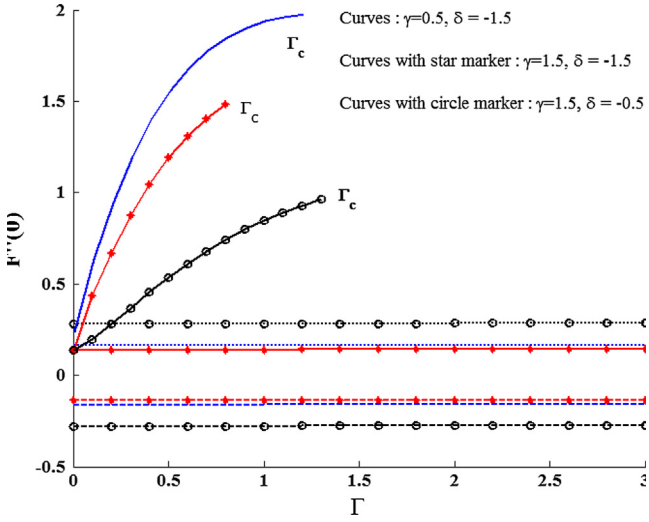

Fig. 6 Variations of $F''(0)$ for different values of Γ, γ and δ when $\phi = 0.05$, $Mn = 0.4$, $s = 2$ and $k_1 = 0.4$. (Dashed lines correspond to stretching sheet, dotted lines correspond to shrinking sheet upper branch solution and solid lines correspond to shrinking sheet lower branch solution).

The solution of Eq. (22) with the corresponding boundary conditions in Eq. (23) in terms of η is obtained as

$$\theta(\eta) = c_{10}\, e^{-\beta\eta\left(\frac{a_0+b_0}{2}\right)}\, M\left(\frac{a_0+b_0-2}{2}, 1+b_0, \frac{-c_8 e^{-\beta\eta}}{\beta}\right) + c_9 e^{-\beta\eta}. \tag{32}$$

where the M is the hypergeometric function [29] defined as following

$$M([a],[b],z) = 1 + \frac{a}{b}z + \frac{a(a+1)}{b(b+1)2!}z^2 + \ldots = \sum_{i=0}^{\infty} \frac{(a)_i}{(b)_i} \frac{z^i}{i!}, \tag{33}$$

and

$$c_7 = c_5\left(s + \frac{d}{\beta(1+\gamma\beta-\delta\beta^2)}\right), \quad c_8 = \frac{c_5 d}{\beta(1+\gamma\beta-\delta\beta^2)}$$

$$c_9 = \frac{St\ c_8}{\left(1-a_0+\frac{c_4\lambda}{\beta^2}\right)\beta}, \quad c_{10} = \frac{1-c_9-St}{M\left(\frac{a_0+b_0-2}{2}, 1+b_0, \frac{-c_8}{\beta}\right)}$$

$a_0 = c_7/\beta$ and $b_0 = \sqrt{a_0^2 - 4\lambda c_4/\beta^2}$.

The quantity of practical interest, in this section the Nusselt number Nu_x which is defined as

$$Nu_x = \frac{\overline{x}\ \overline{q}_w}{k_f(T_w - T_\infty)}, \tag{34}$$

where $\bar{q}_w = -\left(k_{nf} + \frac{16\sigma^* T_\infty^3}{3k_{nf}^*}\right)\left(\frac{\partial T}{\partial \bar{y}}\right)_{\bar{y}=0}$ is the local surface heat flux.

Using (12) and (20) we obtain the following Nusselt number

$$Re_x^{-1/2} Nu_x = \frac{k_{nf}}{k_f}((3N+4)/3N)[-\theta'(0)], \tag{35}$$

where

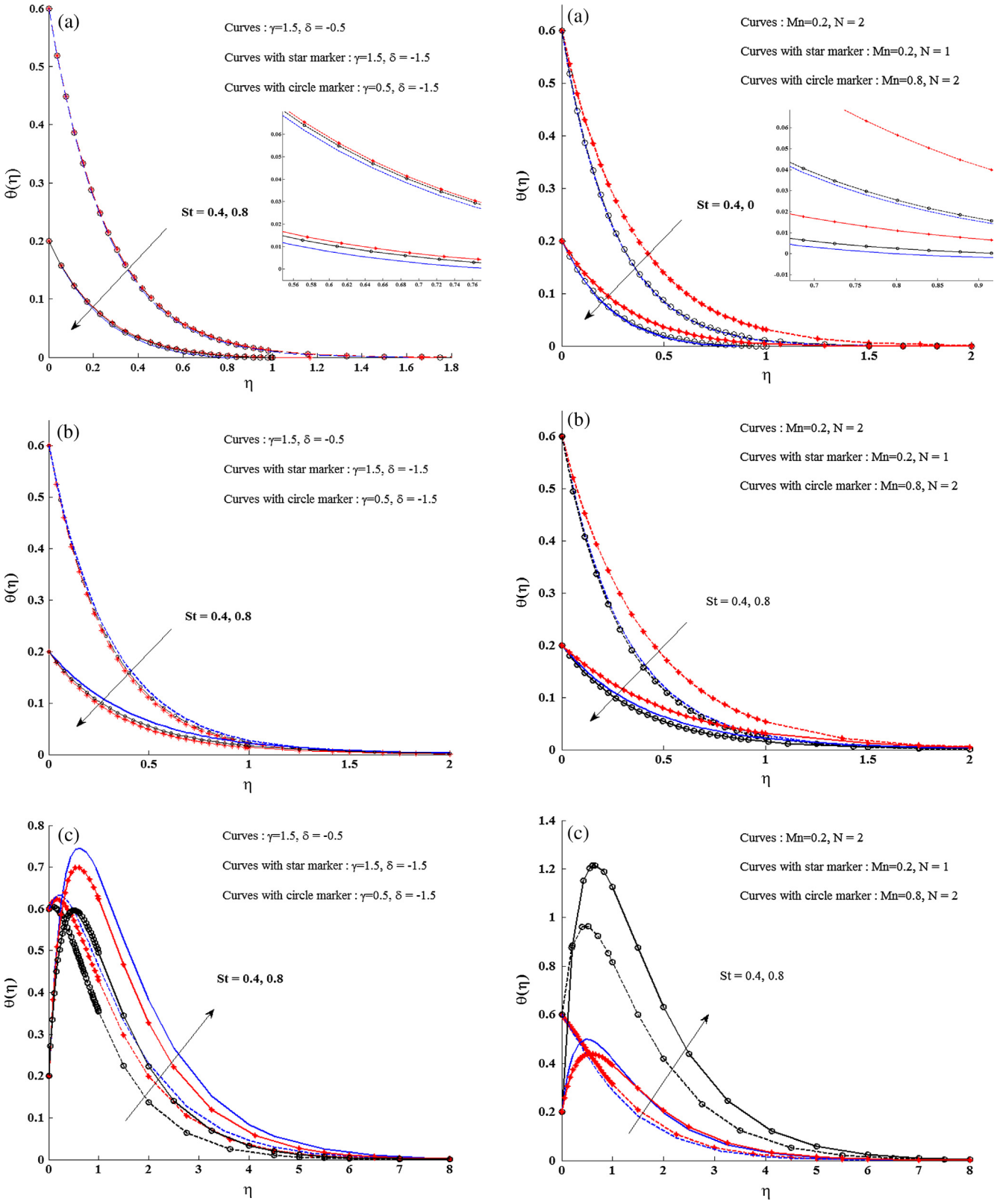

Fig. 7 Effects of first (γ) and second order slip parameters (δ) with stratification parameter on the temperature profile with $s = 1$, $\Gamma = 0.5$, $Mn = 0.4$, $k_1 = 0.4$, $\phi = 0.05$, $\lambda = -0.6$, $Pr = 6.2$, $Ec = 0.5$ and $N = 2$. (a) Stretching sheet ($d = 1$), (b) shrinking sheet upper branch solution ($d = -1$), (c) lower branch solution.

Fig. 8 Effects of magnetic parameter and radiation parameter with stratification parameter on the temperature profile with $s = 1$, $\gamma = 1$, $\delta = 1$, $\Gamma = 0.5$, $k_1 = 0.4$, $\phi = 0.05$, $\lambda = -0.6$, $Ec = 0.5$ and $Pr = 6.2$. (a) Stretching sheet ($d = 1$), (b) shrinking sheet upper branch solution ($d = -1$), (c) lower branch solution.

Table 3a Values of $-\theta'(0)$ for stretching sheet.

		Au	Ag	Cu	Al	Al_2O_3	TiO_2
Γ	0.3	1.44271163	1.46488820	1.49680247	1.50698578	1.52653617	1.32694266
	0.4	1.44262933	1.46469024	1.49656547	1.50658870	1.52616824	1.32656421
	0.5	1.44254773	1.46449468	1.49633149	1.50619736	1.52580557	1.32619115
Mn	0.3	1.44429946	1.46868551	1.50138142	1.51585071	1.53437935	1.33506624
	0.4	1.44340268	1.46652106	1.49876850	1.51081159	1.52991275	1.33044270
	0.5	1.44254773	1.46449468	1.49633149	1.50619736	1.52580557	1.32619115
k_1	0.3	1.44463391	1.46943074	1.50227954	1.51736916	1.53577715	1.33656690
	0.4	1.44356048	1.46686503	1.49918127	1.51149433	1.53054443	1.33112022
	0.5	1.44254773	1.46449468	1.49633149	1.50619736	1.52580557	1.32619115
ϕ	0.05	1.66761864	1.68739051	1.70707758	1.71515508	1.72650387	1.48041289
	0.1	1.44254773	1.46449468	1.49633149	1.50619736	1.52580557	1.32619115
	0.15	1.26214448	1.28224178	1.32179161	1.33068551	1.35639277	1.19415909
γ	0.5	1.44769216	1.47412477	1.50754227	1.52366473	1.54204685	1.34274377
	1	1.44497371	1.46902067	1.50159079	1.51438486	1.53341720	1.33395143
	1.5	1.44254773	1.46449468	1.49633149	1.50619736	1.52580557	1.32619115
δ	−0.5	1.45888867	1.48732480	1.52155398	1.53681770	1.55585303	1.35715183
	−1	1.44955086	1.47448081	1.50735389	1.51984910	1.53913611	1.33992502
	−1.5	1.44254773	1.46449468	1.49633149	1.50619736	1.52580557	1.32619115
Ec	0.3	1.44544829	1.46938042	1.50172834	1.51428529	1.53332004	1.33384440
	0.4	1.44399801	1.46693755	1.49902992	1.51024133	1.52956280	1.33001778
	0.5	1.44254773	1.46449468	1.49633149	1.50619736	1.52580557	1.32619115
N	0.5	0.99395756	1.01023074	1.03054467	1.04088088	1.05251148	0.91299836
	1	1.44254773	1.46449468	1.49633149	1.50619736	1.52580557	1.32619115
	1.5	1.72730962	1.75230020	1.79154457	1.80020426	1.82520920	1.58780126
St	0.4	1.44254773	1.46449468	1.49633149	1.50619736	1.52580557	1.57021818
	0.5	1.20794372	1.23090370	1.25905729	1.27389998	1.28898773	1.32619115
	0.6	0.97333970	0.99731272	1.02178309	1.04160261	1.05216989	1.08216413

Note: While studying the effect of individual parameters the following values are assumed $s = 1$, $d = 1$, $\Gamma = 0.5$, $k_1 = 0.5$, $Mn = 0.5$, $\phi = 0.1$, $\gamma = 1.5$, $\delta = -1.5$, $St = 0.4$, $\lambda = -0.5$, $Ec = 0.5$, $Pr = 6.2$ and $N = 1$.

$$\theta'(0) = c_{10}\left[-\beta\left(\tfrac{a_0+b_0}{2}\right)M\left(\tfrac{a_0+b_0-2}{2}, 1+b_0, \tfrac{-c_8}{\beta}\right) + \tfrac{c_8(a_0+b_0-2)}{2(1+b_0)}M\left(\tfrac{a_0+b_0}{2}, 2+b_0, \tfrac{-c_8}{\beta}\right)\right] - c_9\beta,$$

where $Re_x^{-1/2}Nu_x$ is the reduced Nusselt number.

4. Numerical simulation of the flow field and heat transfer

The nonlinear ordinary differential Eqs. (21) and (22) along with the boundary conditions in Eq. (23) in the presence of local inertial coefficient and the stratification parameter form a two point boundary value problem and are solved using shooting method along with the fourth order Runge–Kutta scheme by converting it into an initial value problem. In this method we have to choose a suitable finite value of $\eta \to \infty$, say η_∞. We set following first order system:

$$\begin{aligned}
y_1' &= y_2,\\
y_2' &= y_3,\\
y_3' &= c_2\left[(1+\Gamma)y_2^2 - y_1y_3\right] + y_2(k_1 + c_1Mn),\\
y_4' &= y_5,\\
y_5' &= c_5(y_2y_4 + y_2St - y_1y_5) - c_4\lambda y_4 - c_4MnEcy_2^2 - c_6Ecy_3^2,
\end{aligned} \tag{36}$$

with the boundary conditions

$$y_1(0) = s, \quad y_2(0) = d + \gamma\, y_3(0) + \delta\, y_3'(0), \quad y_4(0) = 1 - St. \tag{37}$$

To solve (36) with (37) as an initial value problem we must need the values for $y_3(0)$ i.e. $F''(0)$ and $y_5(0)$ i.e. $\theta'(0)$ but no such values are given. The initial guess values for $F''(0)$ and $\theta'(0)$ are chosen and the fourth order Runge–Kutta integration scheme is applied to obtain the solution. Then we compare the calculated values of $F'(\eta)$ and $\theta(\eta)$ at η_∞ with the given boundary conditions $F'(\eta_\infty) = 0$ and $\theta(\eta_\infty) = 0$, and adjust the values of $F''(0)$ and $\theta'(0)$ using the shooting technique to give better approximation for the solution. The process is repeated until we get the results correct up to the desired accuracy of 10^{-8} level, which fulfills the convergence criterion.

5. Results and discussion

To discuss the results, the numerical computations are carried out by employing the above numerical procedure for various values of pertinent parameters for Au–Water. In order to validate the present results, we have compared the values of $-F''(0)$ for stretching sheet and shrinking sheet solution β with those of Turkyilmazoglu [35] for a special case. The comparisons are found to be excellent (Tables 2a and 2b). The effects

Table 3b Values of $-\theta'(0)$ for shrinking sheet upper branch solution.

		Au	Ag	Cu	Al	Al_2O_3	TiO_2
Γ	0.3	1.34920452	1.29996719	1.30882448	1.22056948	1.25939214	1.05314161
	0.4	1.34899188	1.29931860	1.30801735	1.21897775	1.25795268	1.05166644
	0.5	1.34877634	1.29865475	1.30718947	1.21733392	1.25646730	1.05014449
Mn	0.3	1.34568432	1.28949496	1.29565590	1.19173885	1.23417257	1.02712824
	0.4	1.34727671	1.29430375	1.30174066	1.20553583	1.24613989	1.03948088
	0.5	1.34877634	1.29865475	1.30718947	1.21733392	1.25646730	1.05014449
k_1	0.3	1.34437698	1.28534978	1.29037052	1.17889749	1.22322449	1.01593681
	0.4	1.34666771	1.29246574	1.29942758	1.20024647	1.24157438	1.03480887
	0.5	1.34877634	1.29865475	1.30718947	1.21733392	1.25646730	1.05014449
ϕ	0.05	1.51160384	1.46859597	1.47170422	1.41625065	1.43944778	1.18594316
	0.1	1.34877634	1.29865475	1.30718947	1.21733392	1.25646730	1.05014449
	0.15	1.19674141	1.14719756	1.16048167	1.04873966	1.09846151	0.92927602
γ	0.5	1.33240177	1.25979948	1.26049225	1.12950866	1.17748776	0.96960810
	1	1.34160583	1.28229886	1.28770086	1.18191612	1.22442715	1.01743897
	1.5	1.34877634	1.29865475	1.30718947	1.21733392	1.25646730	1.05014449
δ	−0.5	1.28528180	1.20273249	1.20211704	1.08340138	1.12606833	0.91472748
	−1	1.32776927	1.26472770	1.26950034	1.16635463	1.20745632	0.99942585
	−1.5	1.34877634	1.29865475	1.30718947	1.21733392	1.25646730	1.05014449
Ec	0.3	1.35213891	1.30479442	1.31408993	1.22827877	1.26655461	1.06040195
	0.4	1.35045762	1.30172459	1.31063970	1.22280635	1.26151095	1.05527322
	0.5	1.34877634	1.29865475	1.30718947	1.21733392	1.25646730	1.05014449
N	0.5	0.92899315	0.89424927	0.89790731	0.83726173	0.86270836	0.72134113
	1	1.34877634	1.29865475	1.30718947	1.21733392	1.25646730	1.05014449
	1.5	1.61675793	1.55748570	1.56959920	1.46173827	1.50963809	1.26157111
St	0.4	1.34877634	1.29865475	1.30718947	1.21733392	1.25646730	1.29930932
	0.5	1.11442765	1.06382465	1.06794869	0.97952264	1.01480589	1.05014449
	0.6	0.88007897	0.82899456	0.82870791	0.74171137	0.77314447	0.80097966

Note: While studying the effect of individual parameters the following values are assumed $s = 1$, $d = -1$, $\Gamma = 0.5$, $k_1 = 0.5$, $Mn = 0.5$, $\phi = 0.1$, $\gamma = 1.5$, $\delta = -1.5$, $St = 0.4$, $\lambda = -0.5$, $Ec = 0.5$, $Pr = 6.2$ and $N = 1$.

of various physical parameters on $F''(0)$ and the temperature profile are analyzed through Figs. 1–8. for both stretching and shrinking sheets and the reduced Nusselt number is tabulated for different nanofluids in Tables 3a,3b,3c.

Fig. 2 shows the variation of $F''(0)$ with suction/injection, first and second order slip parameters for both stretching ($d = 1$) and shrinking ($d = -1$) sheets. It is found that a unique solution exists for stretching sheet in both suction and injection cases and dual solutions (upper and lower branch) are obtained in shrinking sheet after a certain range of suction parameter. There are no solution existing for shrinking sheet in injection case. The $F''(0)$ values increase with s in stretching sheet and shrinking sheet lower branch solution cases and decrease in shrinking sheet upper branch solution case. The increasing values of first order slip parameter increase the values of $F''(0)$ in stretching sheet and decrease the same in shrinking sheet. The values of $F''(0)$ decrease as second order slip increases in stretching and shrinking sheet lower branch solution and increase with second order slip parameter in shrinking sheet upper branch solution. It is also seen that there exist critical values $s_c(>0)$ for suction. It should be mentioned that for $0 < s < s_c$ the ordinary differential Eq. (21) has no solutions and the full Navier–Stokes and energy equations should be solved. The s_c point decreases with first order slip parameter and increases with second order slip parameter.

The variations of $F''(0)$ with magnetic and porous medium parameters are shown in Figs. 3 and 4 respectively for both stretching and shrinking sheets. It is clear that the increasing values of magnetic (Fig. 3) and porous medium parameters (Fig. 4) increase the values of $F''(0)$ in stretching and shrinking sheet lower branch solution cases and decrease the $F''(0)$ values in shrinking sheet upper branch solution. The first and second order slip parameters have a same trend on $F''(0)$ as discussed in Fig. 2.

The effects of nanoparticle volume fraction and the local inertia coefficient on $F''(0)$ with first and second order slip parameters are respectively displayed in Figs. 5 and 6. It is observed that the increasing values of nanoparticle volume fraction (Fig. 5) and local inertia coefficient (Fig. 6) increase the values of $F''(0)$ in stretching and shrinking sheet lower branch solution cases and decrease the $F''(0)$ in shrinking sheet upper branch solution. It is also observed from Fig. 6, the shrinking sheet lower branch solution exists only up to certain value of local inertia coefficient (say Γ_c). It should be mentioned that the shrinking lower branch solution does not exist beyond Γ_c. It is noted that Γ_c decreases as fist order slip increases and Γ_c increases as second order slip parameter increases.

The combined effect of first, second order slip and stratification parameters on the nanofluid temperature profile is elucidated in Fig. 7. Stratification parameter is the ratio between the free stream temperature and the nanofluid surface temper-

Table 3c Values of $-\theta'(0)$ for shrinking sheet lower branch solution.

		Au	Ag	Cu	Al	Al_2O_3	TiO_2
Γ	0.3	184.19029260	78.65369944	67.83775717	50.04021728	48.18734832	49.83283660
	0.4	188.00155986	76.84674931	65.00962094	37.48677208	40.04626007	42.29769749
	0.5	189.23483317	75.24685527	62.91115199	31.90975045	35.82663685	38.24080921
Mn	0.3	182.10868266	69.10575025	56.80896270	24.86351625	29.28320041	31.53418455
	0.4	185.64793979	72.12815282	59.80175979	28.20087421	32.42171704	34.75819644
	0.5	189.23483317	75.24685527	62.91115199	31.90975045	35.82663685	38.24080921
k_1	0.3	183.49751117	70.18362375	57.83089028	25.62414651	30.12358643	32.42395902
	0.4	186.34834199	72.67579394	60.32189444	28.58334403	32.84973035	35.21197283
	0.5	189.23483317	75.24685527	62.91115199	31.90975045	35.82663685	38.24080921
ϕ	0.05	105.15545641	58.86332022	53.16791032	37.06643755	39.54347352	40.87669637
	0.1	189.23483317	75.24685527	62.91115199	31.90975045	35.82663685	38.24080921
	0.15	260.26481738	85.14069153	67.86339720	27.50999293	31.81582626	34.96009046
γ	0.5	197.98871135	78.81662646	65.69979944	31.54233174	36.25035748	38.88085204
	1.0	193.46779465	76.94111785	64.22646543	31.70935002	36.00355205	38.52069405
	1.5	189.23483317	75.24685527	62.91115199	31.90975045	35.82663685	38.24080921
δ	0.5	165.00187245	66.08413699	55.97475641	34.60422318	35.85436648	37.60851173
	−1.0	181.99957296	72.23958066	60.56086176	32.52160281	35.61206410	37.81575900
	−1.5	189.23483317	75.24685527	62.91115199	31.90975045	35.82663685	38.24080921
Ec	0.3	113.90158456	45.56183521	38.21471240	20.29321394	22.38040004	23.79358715
	0.4	151.56820891	60.40433868	50.56293214	26.10148160	29.10351860	31.01719821
	0.5	189.23483317	75.24685527	62.91115199	31.90975045	35.82663685	38.24080921
N	0.5	107.59608673	43.43898410	36.67867608	19.49282375	21.67016835	23.20943918
	1	189.23483317	75.24685527	62.91115199	31.90975045	35.82663685	38.24080921
	1.5	243.83256626	95.37046278	79.22204981	39.09020727	44.18188203	47.15408685
St	0.4	189.23483317	75.24685527	62.91115199	31.90975045	35.82663685	38.24080921
	0.5	190.37352473	76.64133524	64.43014886	33.99834951	37.76272308	40.22096365
	0.6	191.51221613	78.03582816	65.94914582	36.08694893	39.69880877	42.20111801

Note: While studying the effect of individual parameters the following values are assumed $s = 4$, $d = -1$, $\Gamma = 0.5$, $k_1 = 0.5$, $Mn = 0.5$, $\phi = 0.1$, $\gamma = 1.5$, $\delta = -1.5$, $St = 0.4$, $\lambda = -0.5$, $Pr = 6.2$, $N = 1$ and $Ec = 0.5$.

ature. The temperature profile of Au–Water decreases with the increasing values of stratification parameter in stretching sheet (Fig. 7(a)). The increase in stratification parameter indicates an increase in free stream temperature or reduction in fluid surface temperature. Thus the increase in stratification parameter leads to thinning of the thermal boundary layer. A similar trend has been observed in shrinking sheet upper branch solution (Fig. 7(b)). But the stratification parameter shows an opposing trend in shrinking sheet lower branch solution. The increasing values of first order slip parameter enhance the temperature profile in stretching and shrinking sheet lower branch solution and reduce the temperature in shrinking sheet upper branch solution. The presence of second order slip decreases the temperature profile in stretching sheet and shrinking sheet lower branch solution and increases in shrinking sheet upper branch solution.

The combined effect of magnetic, radiation and stratification parameters on the temperature of the Au–Water is shown in Fig. 8. It is obvious that the increasing values of magnetic parameter lead to increase the thickness of nanothermal boundary layer in stretching and shrinking sheet lower branch solution (Fig. 8(a) and (c)). This is due to the fact that, when a transverse magnetic field is applied to an electrically conducting fluid, it gives rise to a resistive force, known as the Lorentz force. This force makes the fluid to experience a resistance by increasing the friction between its layers and due to which there is a decrease in velocity and concentration. The temperature increases in the boundary layer due to the Ohmic dissipation effect. But the thermal boundary layer thickness reduces in the presence of magnetic field in shrinking sheet upper branch solution (Fig. 8(c)). It is interesting to note that the increasing values of magnetic parameter increase the temperature profile drastically in shrinking sheet lower branch solution case. The occurrence of radiation parameter always leads to thinning of the nanothermal boundary layer.

The combined effect of Eckert number and nanoparticle volume fraction parameter on the temperature profile is illustrated in Fig. 9. It is noted that the increasing values of Eckert number lead to increase the temperature profile in both stretching (Fig. 9(a)) and shrinking sheets (Fig. 9(b) and (c)). Due to the fact that the viscous dissipation produces heat due to drag between the nanofluid particles and this extra heat causes an increase in the initial fluid temperature. The presence of viscous dissipation leads to increase the nanothermal boundary layer thickness. The temperature profile increases with the increase in nanoparticle volume fraction in stretching sheet and shrinking upper branch solution case and an opposite trend has been noted in shrinking sheet lower branch solution case. The stratification parameter shows the same effect as discussed in Fig. 7.

Please cite this article in press as: Vishnu Ganesh N et al., Darcy–Forchheimer flow of hydromagnetic nanofluid over a stretching/shrinking sheet in a thermally stratified porous medium with second order slip, viscous and Ohmic dissipations effects, Ain Shams Eng J (2016), http://dx.doi.org/10.1016/j.asej.2016.04.019

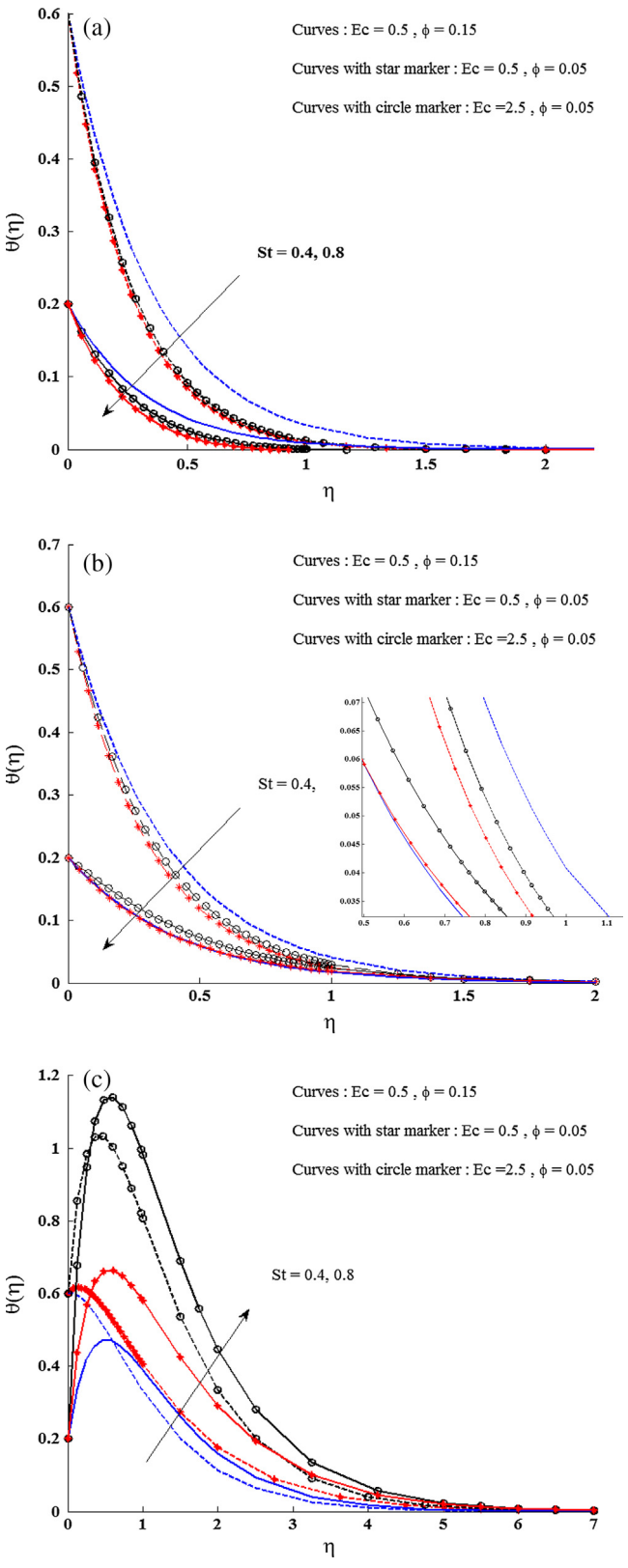

Fig. 9 Effects of Eckert number and nanoparticle volume fraction parameter with stratification parameter on the temperature profile with $s = 1$, $\gamma = 1$, $\delta = 1$, $\Gamma = 0.5$, $k_1 = 0.4$, $Mn = 0.4$, $\lambda = -0.6$, $Ec = 0.5$, $N = 2$ and $Pr = 6.2$. (a) Stretching sheet ($d = 1$), (b) shrinking sheet upper branch solution ($d = -1$), (c) lower branch solution.

6. Conclusion

We have studied the second order slip flow of a nanofluid over stretching/shrinking sheet embedded in a thermally stratified porous medium in the presence of viscous and Ohmic dissipations effects. The governing equations of the problem are converted into ordinary differential equations by using scaling transformations. The transformed equations are solved numerically by fourth order Runge–Kutta method with shooting technique. Following conclusions can be derived from the present results.

- A unique solutions exist for stretching sheet in both suction and injection cases. Dual solutions are obtained beyond a suction critical point. The shrinking sheet solution does not exist in injection case. The increasing value of first order slip parameter decreases the suction critical point and the second order slip parameter shows an opposite effect on suction critical point.
- The lower branch solution exists only for the certain range of local inertia coefficient. The increasing value of first order slip parameter decreases the local inertia critical point and the second order slip parameter shows an opposite effect on local inertia critical point.
- The temperature profile increases in the presence of viscous dissipation in both stretching and shrinking sheets.
- The increasing values of stratification parameter lead to thinning of the thermal boundary layer in stretching and shrinking sheet upper branch solution case and an opposite behavior is observed in shrinking sheet lower branch solution.
- The presence of second order slip decreases the temperature profile in stretching sheet and shrinking sheet lower branch solution and increases in shrinking sheet upper branch solution.
- The nanothermal boundary layer thickness increases in stretching and shrinking sheet lower branch solution and decreases in shrinking sheet upper branch solution in the presence of Ohmic dissipation.
- The existence of thermal radiation decreases the thermal boundary layer thickness in both stretching and shrinking sheets.

Acknowledgments

The authors wish to express their sincere thanks to the honorable referees and the editor for their valuable comments and suggestions to improve the quality of the paper. One of the authors (N.V.G) gratefully acknowledges the financial support of Rajiv Gandhi National Fellowship (RGNF), UGC, New Delhi, India.

References

[1] Abu-Nada E, Masoud Z, Hijazi A. Natural convection heat transfer enhancement in horizontal concentric annuli using nanofluids. Int Commun Heat Mass Transfer 2008;35:657–65.
[2] Kuznetsov AV, Nield DA. Natural convective boundary-layer flow of a nanofluid past a vertical plate. Int J Therm Sci 2010;49:243–7.

[3] Van Gorder RA, Sweet E, Vajravelu K. Nano boundary layers over stretching surfaces. Commun Nonlinear Sci Numer Simulat 2010;15:494–500.
[4] Vajravelu K, Prasad KV, Lee Jinho, Lee Changhoon, Pop I, Robert Van Gorder A. Convective heat transfer in the flow of viscous Ag–water and Cu–water nanofluids over a stretching surface. Int J Therm Sci 2011;50:843–51.
[5] Rashidi MM, Beg O, Asadi M, Rastegari MT. DTM-Padé modeling of natural convective boundary layer flow of a nano fluid past a vertical surface. Int J Therm Environ Eng 2011;4 (1):13–24.
[6] Rashidi MM, Erfani E. The modified differential transform method for investigating nano boundary-layers over stretching surfaces. Int J Numer Meth Heat Fluid Flow 2011;21(7): 864–83.
[7] Hady FM, Ibrahim1 FS, Abdel-Gaied SM, Eid MR. Radiation effect on viscous flow of a nanofluid and heat transfer over a nonlinearly stretching sheet. Nanoscale Res Lett 2012;7:229–42.
[8] Turkyilmazoglu M, Pop I. Heat and mass transfer of unsteady natural convection flow of some nanofluids past a vertical infinite flat plate with radiation effect. Int J Heat Mass Transfer 2013;59:167–71.
[9] Rashidi MM, Abelman S, Freidoonimehr N. Entropy generation in steady MHD flow due to a rotating porous disk in a nanofluid. Int J Heat Mass Transfer 2013;62:515–25.
[10] Vishnu Ganesh N, Ganga B, Abdul Hakeem AK. Lie symmetry group analysis of magnetic field effects on free convective flow of a nanofluid over a semi infinite stretching sheet. J Egypt Math Soc 2014;22:304–10.
[11] Vishnu Ganesh N, Abdul Hakeem AK, Jayaprakash R, Ganga B. Analytical and numerical studies on hydromagnetic flow of water based metal nanofluids over a stretching sheet with thermal radiation effect. J Nanofluids 2014;3:154–61.
[12] Rashidi MM, Momoniat E, Mohammad F, Basiri Parsa A. Lie group solution for free convective flow of a nanofluid past a chemically reacting horizontal plate in porous media. Math Probl Eng 2014 239082.
[13] Rashidi MM, Vishnu Ganesh N, Abdul Hakeem AK, Ganga B. Buoyancy effect on MHD flow of nanofluid over a stretching sheet in the presence of thermal radiation. J Mol Liq 2014;198:234–8.
[14] Haq R, Nadeem S, Khan ZH, Akbar NS. Thermal radiation and slip effects on MHD stagnation point flow of nanofluid over a stretching sheet. Physica E 2015;65:17–23.
[15] Das S, Jana RN, Makinde OD. Mixed convective magnetohydrodynamic flow in a vertical channel filled with nanofluids. Eng Sci Technol Int J 2015;18(2):244–55.
[16] Das S, Banu AS, Jana RN, Makinde OD. Entropy analysis on MHD pseudo-plastic nanofluid flow through a vertical porous channel with convective heating. Alex Eng J 2015;54(3):325–37.
[17] Khamis S, Makinde OD, Nkansah-Gyekye Y. Buoyancy – driven heat transfer of water based nanofluid in a permeable cylindrical pipe with Navier slip through a saturated porous medium. J Porous Media 2015;18(12):1169–80.
[18] Das S, Chakraborty S, Jana RN, Makinde OD. Entropy analysis of unsteady magneto-nanofluid flow past accelerating stretching sheet with convective boundary condition. Appl Math Mech 2015;36(12):1593–610.
[19] Hussain T, Hayat T, Shehzad SA, Alsaedi A, Chen B. A model of solar radiation and joule heating in flow of third grade nanofluid. Z Naturforsch A 2015;70(3):177–84.
[20] Shehzad SA, Abdullah Z, Alsaedi A, Abbasi FM, Hayat T. Thermally radiative three-dimensional flow of Jeffrey nanofluid with internal heat generation and magnetic field. J Magn Magn Mater 2016;397(1):108–14.
[21] Shehzad SA, Abdullah Z, Abbasi FM, Hayat T, Alsaedi A. Magnetic field effect in three-dimensional flow of an Oldroyd-B nanofluid over a radiative surface. J Magn Magn Mater 2016;399 (1):97–108.
[22] Vishnu Ganesh N, Abdul Hakeem AK, Ganga B. A comparative theoretical study on Al_2O_3 and γ-Al_2O_3 nanoparticles with different base fluids over a stretching sheet. Adv Powder Technol 2016. http://dx.doi.org/10.1016/j.apt.2016.01.015.
[23] Nield DA, Bejan A. Convection in porous media. Springer Verlag; 1992.
[24] Pal D, Mondal H. Effects of Soret Dufour, chemical reaction and thermal radiation on MHD non-Darcy unsteady mixed convective heat and mass transfer over a stretching sheet. Commun Nonlinear Sci Numer Simulat 2011;16:1942–58.
[25] Pal D, Mondal H. Effects of temperature-dependent viscosity and variable thermal conductivity on MHD non-Darcy mixed convective diffusion of species over a stretching sheet. J Egypt Math Soc 2014;22:123–33.
[26] Anwar Bég O, Zueco J, Takhar HS. Laminar free convection from a continuously-moving vertical surface in thermally-stratified non-Darcian high-porosity medium: network numerical study. Int Commun Heat Mass Transfer 2008;35:810–6.
[27] Shehzad SA, Hayat T, Alhuthali MS, Asghar S. MHD three-dimensional flow of Jeffrey fluid with Newtonian heating. J Central South Univ 2014;21(4):1428–33.
[28] Hayat T, Shehzad SA, Alsaedi A. MHD three-dimensional flow of Maxwell fluid with variable thermal conductivity and heat source/sink. Int J Numer Meth Heat Fluid Flow 2014;24(5):1073–85.
[29] Anjali Devi SP, Ganga B. Effects of viscous and Joules dissipation on MHD flow, heat and mass transfer past a stretching porous surface embedded in a porous medium. Nonlinear Anal: Model Control 2009;14:303–14.
[30] Motsumi TG, Makinde OD. Effects of thermal radiation and viscous dissipation on boundary layer flow of nanofluids over a permeable moving flat plate. Phys Scr 2012;86:045003.
[31] Makinde OD, Mutuku WN. Hydromagnetic thermal boundary layer of nanofluids over a convectively heated flat plate with viscous dissipation and Ohmic heating. UPB Sci Bull Series A 2014;76:181–92.
[32] Ganga B, Ansari SMY, Vishnu Ganesh N, Abdul Hakeem AK. MHD radiative boundary layer flow of nanofluid past a vertical plate with internal heat generation/absorption, viscous and Ohmic dissipation effects. J Nigerian Math Soc 2015;34:181–94.
[33] Fang T, Yao S, Zhang J, Aziz A. Viscous flow over a shrinking sheet with second order slip flow model. Commun Nonlinear Sci Numer Simulat 2010;15:1831–42.
[34] Nandeppanavar MM, Vajravelu K, Abel MS, Siddalingappa MN. Second order slip flow and heat transfer over a stretching sheet with non-linear Navier boundary condition. Int J Therm Sci 2012;58:143–50.
[35] Turkyilmazoglu M. Heat and mass transfer of MHD second order slip flow. Comput Fluids 2013;71:426–34.
[36] Singh G, Chamka AJ. Dual solutions for second order slip flow and heat transfer on a vertical permeable shrinking sheet. Ain shams Eng J 2013;4(4):911–7.
[37] Rosca NC, Pop I. Boundary layer flow past a permeable shrinking sheet in a micropolar fluid with a second order slip flow model. Eur J Mech B – Fluid 2014;48:115–22.
[38] Abdul Hakeem AK, Vishnu Ganesh N, Ganga B. Magnetic field effect on second order slip flow of nanofluid over a stretching/shrinking sheet with thermal radiation effect. J Magn Magn Mater 2015;381:243–57.
[39] Abdul Hakeem AK, Vishnu Ganesh N, Ganga B. Effect of heat radiation in a Walter's liquid B fluid over a stretching sheet with non-uniform heat source/sink and elastic deformation. J King Saud Univ – Eng Sci 2014;26:168–75.
[40] Domkundwar AV, Dom dundwar VM. Heat and mass transfer data book. Delhi: Dhanpa Rai and Co (p) Ltd., Educational and Technical Publishers; 2004.

Please cite this article in press as: Vishnu Ganesh N et al., Darcy–Forchheimer flow of hydromagnetic nanofluid over a stretching/shrinking sheet in a thermally stratified porous medium with second order slip, viscous and Ohmic dissipations effects, Ain Shams Eng J (2016), http://dx.doi.org/10.1016/j.asej.2016.04.019

N. Vishnu Ganesh is a research scholar in Department of Mathematics in Sri Ramakrishna Mission Vidyalaya College of Arts and Science, Coimbatore, Tamil Nadu, India. He is currently doing Ph.D with F1-17.1/2012-13/RGNF-2012-13-SC-TAM-16936 UGC grant India under the guidance of DR. A.K. Abdul Hakeem.

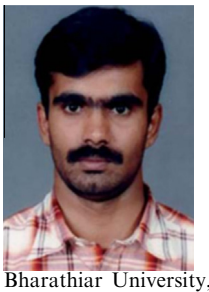

A.K. Abdul Hakeem was born and brought up in the district of Coimbatore, Tamil Nadu, India. He obtained the M.Sc. and M.Phil degrees in Mathematics from Bharathiar University, Coimbatore. He was awarded Ph. D. degree in Fluid Dynamics by the Bharathiar University in 2008. He is serving the Department of Mathematics, the Sri Ramakrishna Mission Vidhyalaya College of Arts and Science, Coimbatore Affiliated to Bharathiar University, as an Assistant Professor since 2008. Besides teaching he is actively engaged in research in the field of Fluid mechanics particularly in Heat transfer in cavities, boundary layer flows, Nanofluid Flow through Porous media and Slip flow model.

B. Ganga was born and brought up in the district of the Nilgiris, Tamil Nadu, India. She obtained M.Phil and Ph.D degrees in Mathematics from Bharathiar University, Coimbatore. She is currently working as an Assistant Professor in Department of Mathematics, Providence College for Women, Coonoor, Affiliated to Bharathiar University since 2007. Besides teaching she is actively engaged in research in the field of Fluid mechanics particularly in boundary layer flows, Nanofluid Flow through Porous media and Slip flow model.

Please cite this article in press as: Vishnu Ganesh N et al., Darcy–Forchheimer flow of hydromagnetic nanofluid over a stretching/shrinking sheet in a thermally stratified porous medium with second order slip, viscous and Ohmic dissipations effects, Ain Shams Eng J (2016), http://dx.doi.org/10.1016/j.asej.2016.04.019